

Laser spectroscopy of ion-size effects on point-defect equilibria in  $\text{PbF}_2:\text{Eu}^{3+}$ 

Forrest J. Weesner and John C. Wright\*

*Department of Chemistry, University of Wisconsin, Madison, Wisconsin 53706*

John J. Fontanella

*Physics Department, U.S. Naval Academy, Annapolis, Maryland 21402*

(Received 22 July 1985)

Recent experiments have suggested a change occurs in the type of defects present in  $\text{PbF}_2$  when trivalent lanthanide ions larger than gadolinium are doped in the crystals. Site-selective spectroscopy has been used to study  $\text{PbF}_2:\text{Eu}^{3+}$  as an example of such a system. It is found that the types of defects and the behavior of the site distribution are very similar to those of the smaller ions. In particular, there is no evidence for an electron-compensated site. It is found that there are only two important sites at low concentrations, a cubic site and a single-pair site. The single-pair site is shown to correlate with the dielectric relaxation peak observed for  $\text{PbF}_2:\text{Eu}^{3+}$ . Clustering becomes important at higher concentrations. There is extensive dissociation of the locally compensated defect sites near the superionic transition temperature that is direct evidence for the importance of strain interactions causing large nonideality corrections in the defect equilibria. The nonidealities also may prevent one from using unique values for the site association energies.

## INTRODUCTION

$\text{PbF}_2$  is a particularly interesting member of the fluorites because many of its properties are different from the other members of the series, particularly the low transition temperature for superionic conductivity.<sup>1-5</sup> Dielectric relaxation measurements have shown that the site distribution in  $\text{PbF}_2$  doped with trivalent lanthanides is a sharp function of the dopant size.<sup>1,6-8</sup> Dopants smaller than Gd have a number of relaxations that are attributed to clusters and single pairs that are lanthanide ions compensated locally by a fluoride interstitial ion ( $\text{Eu}_{\text{Pb}}\cdot\text{F}_i$ )<sup>x</sup>.  $\text{Gd}^{3+}$  and larger ions appear to have a very different site distribution with only one peak in the dielectric relaxation spectrum. This peak has a number of unusual properties.<sup>1</sup> The energy of the peak is strongly dependent on the ionic size, a behavior that was observed only for sites associated with clusters in the alkaline-earth fluorides.<sup>9-11</sup> Since the peak is the only significant feature in the dielectric relaxation down to very low dopant concentrations, it was attributed to a single pair and not a cluster.<sup>1</sup> Such an assignment is unexpected since there has not been an ion-size-dependent relaxation observed for a single pair defect in any of the other fluorites. A particularly striking property of the relaxation peak was the relaxation time decreased as the pressure was increased, a feature that had not been observed previously in any sample.<sup>12-15</sup> Finally, the conductivity did not scale with the size of the relaxation so the defect that corresponded to the relaxation could not be contributing appreciably to the conductivity. These unusual properties were attributed either to an electron-compensated lanthanide site or a fluoride-interstitial-compensated site with a large value for the association energy so the site could not contribute to the conductivity measured in the dielectric relaxation.<sup>1</sup> The fluoride-compensated site would need to have a soft

local-phonon mode in order to explain the size and pressure dependence. Either explanation required an additional fluoride-compensated site that was invisible in the dielectric relaxation to explain the fact that the bulk electrical conductivity could be fitted by a classical association model.<sup>16,17</sup> The electron-compensated model was favored because it would not contribute to the conductivity which is primarily ionic in  $\text{PbF}_2$  and it would not have a problem explaining the low activation energy for the dielectric relaxation peak in  $\text{Gd}^{3+}$ . It would also be consistent with the reports of a small electronic contribution to the conductivity.<sup>16</sup>

Site-selective laser spectroscopy has been quite successful in studying the defect distributions in doped insulators since it is sensitive to all of the sites that contain lanthanides and it has the selectivity required to resolve the contributions of the individual sites, even with complex distributions.<sup>18-23</sup> Such methods were used to look at  $\text{PbF}_2:\text{Er}^{3+}$ , an example of an ion smaller than Gd.<sup>24</sup> The site distribution was very similar to that observed in the alkaline-earth fluorides. Three locally compensated single  $\text{Er}^{3+}$  sites, three sites associated with clusters, and a distantly compensated cubic site were observed. The cubic site was seen to increase in importance as the total dopant concentration was increased. This behavior is not in agreement with defect equilibrium models based on mass action relationships but is similar to the anomalous behavior observed in the alkaline-earth fluorides.<sup>20</sup> The alkaline-earth fluorides also exhibited an anomalous dependence on the annealing temperature.<sup>23</sup> The cubic site decreased in concentration as the annealing temperature was raised whereas classical equilibrium models predict that associated pairs and clusters will dissociate to form cubic sites at sufficiently high temperature. It is important to note also that  $\text{Eu}^{3+}$  and  $\text{Er}^{3+}$  had the same behavior in all of the alkaline-earth fluorides studied pre-

viously, and there is no indication that the ease with which  $\text{Eu}^{3+}$  can be reduced has any influence on the site distribution.<sup>18,19,21,24</sup>  $\text{PbF}_2:\text{Er}^{3+}$ , however, did not show the anomalous temperature dependence.<sup>25</sup> The cubic site increased with temperature with a very rapid increase near the superionic transition temperature. The rapid increase was a direct indication of the importance of nonideality corrections in controlling the site distribution and the superionic transition itself.

In this paper, we use site-selective laser spectroscopy of  $\text{PbF}_2:\text{Eu}^{3+}$  to look for evidence of the electron-compensated site or other indications of an unusual site distribution. This system is representative of the  $\text{PbF}_2$  systems that have only one peak in the dielectric relaxation. The types of sites are identified and the site distribution is studied as a function of the dopant concentration and annealing temperature. Despite the big differences seen in the dielectric relaxation between Er and Eu, the site-selective spectroscopy shows the systems are quite similar. The Eu system has one site associated with a locally compensated Eu site,  $(\text{Eu}_{\text{Pb}}\cdot\text{F}_i)^x$ , a single Eu in a cubic site, five sites associated with clustering, and a number of minor sites. At low concentrations, only the cubic site and the  $(\text{Eu}_{\text{Pb}}\cdot\text{F}_i)^x$  site are important. The  $(\text{Eu}_{\text{Pb}}\cdot\text{F}_i)^x$  site is shown to correspond to the single dielectric peak observed earlier. This site dissociates to form the cubic site with the same strong temperature dependence seen in the Er system around the superionic transition temperature. If the site corresponded to an electron-compensated site, there would have to be a large contribution from electronic conduction in  $\text{PbF}_2:\text{Eu}^{3+}$ . Thus we find no evidence that this site is electron compensated. There is also no indication of another site that would have the properties of an electron-compensated site. If the dopant concentration is raised from 0.1 to 1.0 mol %, clustering becomes important and the spectrum increases in complexity. The cubic site exhibits the same anomalous increase with dopant concentration observed in the other systems.

## EXPERIMENTAL

$\text{PbF}_2$  single crystals containing nominally 0.01, 0.1, and 1 mol %  $\text{Eu}^{3+}$  were used in this study. The crystals were grown by the Stockbarger technique. The dopant concentrations were determined by neutron activation to be 0.020, 0.137, and 1.01 mol %, respectively. The absorption spectrum was measured to find indications of the presence of  $\text{Eu}^{2+}$ . There was a small and gradual increase in absorption in most samples until the 260-nm cutoff.  $\text{Eu}^{2+}$  absorption was observed only in the 1-mol % sample where it is estimated to represent less than 10% of the total Eu.

All experiments were performed at 14 K using a closed-cycle cryogenic refrigerator.  $\text{Eu}^{3+}$  fluorescence was excited by a nitrogen laser pumped dye laser with a typical bandwidth of 0.025 nm. The fluorescence was collected and directed into either a low-resolution  $\frac{1}{4}$ -m monochromator to monitor fluorescence from all  $\text{Eu}^{3+}$  sites or into a high-resolution 1-m monochromator to observe transitions of individual sites. Absorption measurements were made using a tungsten-halogen lamp and the

1-m monochromator. Details of the spectroscopic system and site-selective methods have been previously described.<sup>26</sup>

The temperature dependence of the site distribution was established by annealing the crystals at the selected temperature followed by a rapid quench to preserve the high-temperature distribution. The crystals were sealed in evacuated Vycor tubes in the presence of lead fluoride powder and placed into a preheated furnace for annealing. Following an appropriate equilibration period, ranging from 6 h (650°C) to 3 d (350°C), the sealed tubes were removed from the furnace and cooled by immersion in flowing tap water.

## RESULTS AND DISCUSSION

### Site classification

Absorption spectra are valuable in determining the site distribution because they show all the major sites, including ones that may not fluoresce. The absorption spectra of the  ${}^7F_0 \rightarrow {}^5D_1$  transition in the 0.01- and 0.1-mol % crystals are shown in Fig. 1. This spectrum has been previously reported by Findley *et al.*<sup>27</sup> The doublet observed in their experiment is actually an unresolved triplet as shown in Fig. 1. The strong central line is assigned to the distantly compensated cubic site, labeled C, and the remaining doublet is assigned to a site labeled A. These two are the only important sites below approximately 0.2 mol %. We do observe an additional unidentified weak absorption as a shoulder on the long-wavelength line of the A-site doublet in the 0.1-mol % sample. It is not observed in any of the other samples including those annealed at different temperatures.

Excitation spectra of the crystals before annealing appear in Fig. 2 for three different concentrations. Both  ${}^7F_0 \rightarrow {}^5D_0$  and  ${}^7F_0 \rightarrow {}^5D_1$  excitation spectra are shown for comparison. Fourteen  $\text{Eu}^{3+}$  sites have been identified in  $\text{PbF}_2:\text{Eu}^{3+}$  over the concentration range studied. The in-

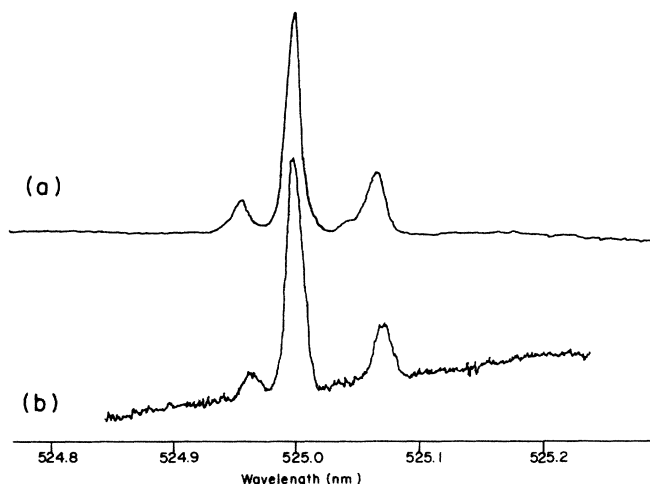


FIG. 1. Absorption spectra of the  ${}^7F_0 \rightarrow {}^5D_1$  transition of  $\text{PbF}_2$  doped with (a) 0.1 and (b) 0.01 mol %  $\text{Eu}^{3+}$ .

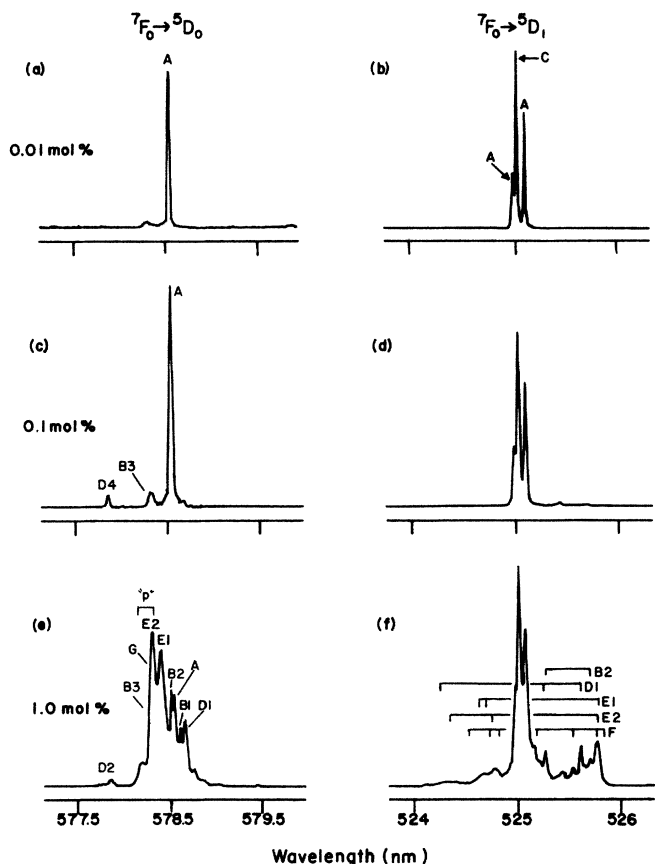


FIG. 2.  ${}^7F_0 \rightarrow {}^5D_0$  and  ${}^7F_0 \rightarrow {}^5D_1$  excitation spectra of unannealed crystals when all fluorescence above 580 nm is monitored. (a) and (b)  $\text{PbF}_2:0.01 \text{ mol } \% \text{ Eu}^{3+}$ . (c) and (d)  $\text{PbF}_2:0.1 \text{ mol } \% \text{ Eu}^{3+}$ . (e) and (f)  $\text{PbF}_2:1.0 \text{ mol } \% \text{ Eu}^{3+}$ .

dividual fluorescence and excitation spectra for each site are shown in Figs. 3–7. Several other sites are present but spectral congestion prevented assignment of several lines in the  ${}^7F_0 \rightarrow {}^5D_1$  excitation spectrum. The various  $\text{Eu}^{3+}$  sites in  $\text{PbF}_2:\text{Eu}^{3+}$  were grouped into two broad categories—those consisting of a single europium ion,

TABLE I. Fluorescence lifetimes for Eu sites in  $\text{PbF}_2$ . All values are in milliseconds except as noted. \* denotes too short to measure.

Site label	${}^5D_1$	${}^5D_0$
A	5.07	6.02
B1	3.74	7.90
B2	3.34	8.09
B3	5.00	9.45
C	7.60	9.75
D1	87 $\mu\text{s}$	4.77
D2	120 $\mu\text{s}$	4.80
E1	35 $\mu\text{s}$	5.17
E2	38 $\mu\text{s}$	5.14
F	40 $\mu\text{s}$	5.15
G	1.68	3.12
H1	6.5	10
H2	6.75	10
S	*	8.58

charge compensated either locally or distantly, and those associated with clustering of two or more europium ions. Two criteria were used to classify each site. First, the contribution to the fluorescence spectrum from sites involved in clustering is expected to increase in importance with total dopant concentration. Second, the  ${}^5D_1$  manifold of a  $\text{Eu}^{3+}$  ion within a cluster can relax efficiently by energy transfer to neighboring  $\text{Eu}^{3+}$  ions. Thus the distinction between single-ion and cluster sites was based on observations of relative fluorescence intensity as a function of concentration and the differences in the  ${}^5D_1$  lifetimes. The site labels and fluorescent lifetimes appear in Table I. Rare-earth ions in clusters often display more transitions between  $J$  manifolds than is possible for a single ion. This property has been useful in classifying ion sites in some systems,<sup>23</sup> but did not prove useful in this

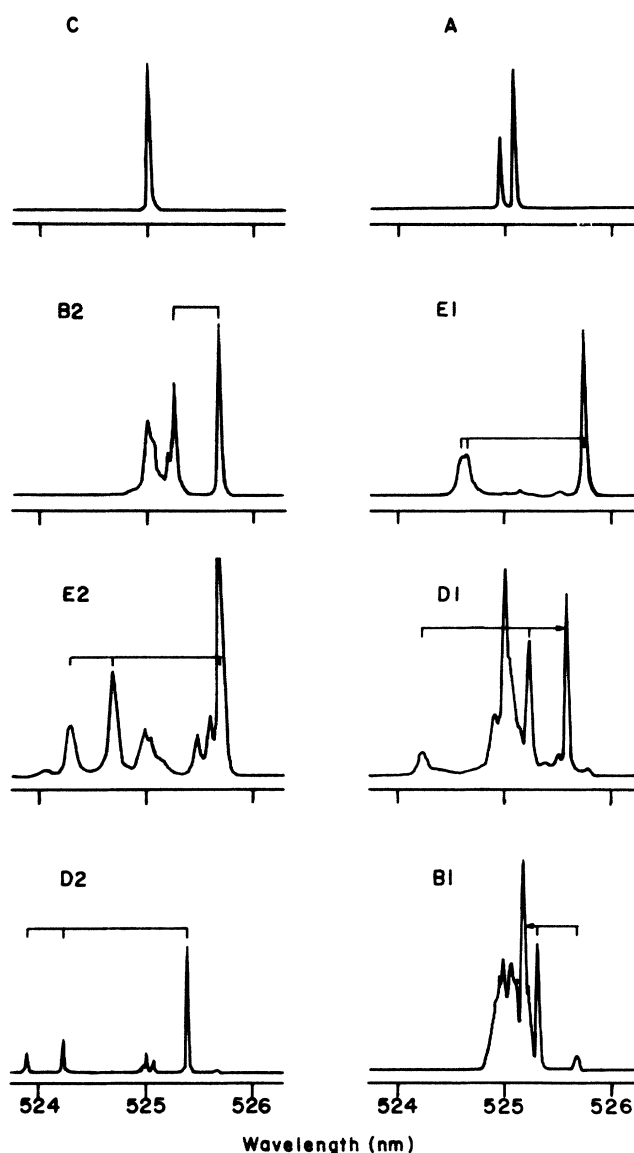


FIG. 3.  ${}^7F_0 \rightarrow {}^5D_1$  excitation spectra of the important sites in  $\text{PbF}_2:\text{Eu}^{3+}$  monitoring the following wavelengths: site C, 584.5 nm; site A, 584.1 nm; site B2, 533.2 nm; site E1, 650.5 nm; site E2, 586.4 nm; site D1, 588.1 nm; site D2, 588.4 nm; site B1, 535.0 nm.

study because only one site clearly exceeded the maximum  $2J+1$  splitting of an energy term allowed for a non-Kramers ion. Using these criteria the *A*, *B1*, *B2*, *B3*, *C*, *G*, *H1*, and *H2* sites are classified as single-ion sites and *D1*, *D2*, *E1*, *E2*, *F*, and *S* as sites associated with clusters.

Only the *A* and *C* sites are of importance in the 0.1-mol% or lower crystals. Excitation and fluorescence spectra for these sites appear at the top of Figs. 3 and 4. The *C* site is the most important feature. It has a long  $^5D_1$  lifetime indicating that it is a single-ion site. The fluorescence spectrum has the least number of transitions of any site and corresponds to the number of levels expected for octahedral symmetry. The intensity of the different transitions follows the selection rules for magnetic dipole transitions in an octahedral field. These observations lead us to assign the *C* site to the distantly compensated site of cubic symmetry. The *C* site has intense phonon bands peaking at about 90, 190, and 270  $\text{cm}^{-1}$  from the electronic transition origins. The presence of this phonon structure over larger regions of the spectrum often prevented discrimination against the *C* site in selective excitation spectra of other sites. Since the *C* site cannot be observed in a dielectric relaxation experiment, the *A* site must be responsible for the principal relaxation seen in the dielectric spectrum because it is the only other important site at or below 0.1 mol%. The energy levels for the *C* and *A* sites are presented in Fig. 5.

The  $^7F_2$  and  $^7F_3$  levels of the *A* site deviate noticeably from those of the cubic site. If the *A* site is compensated

by an electron localized on an adjacent lattice fluorine,  $C_{3v}$  point-group symmetry would result. Local compensation by a fluoride interstitial ( $F_i'$ ) would also be expected to produce a site with  $C_{3v}$  symmetry since the next-nearest-neighbor position would be favored for the Eu to Pb size ratio.<sup>28</sup> The crystal-field splittings are consistent with a  $C_{3v}$  point-group symmetry site but cannot be considered definitive evidence. The  $^5D_0$  and  $^5D_1$  levels of the *A* site also have the long lifetimes characteristic of a single-pair site.

There are a large number of sites that exist at higher dopant concentrations. Some of the new sites are single-pair sites and are labeled *B1*, *B2*, and *B3*. The  $^5D_1$  and  $^5D_0$  manifolds have long fluorescent lifetimes. The *B* sites are present in the 0.1-mol% crystals as minor sites but are difficult to selectively excite due to the much stronger lines from the *C* and *A* sites. Selected spectra of these sites appear in Figs. 3, 4, and 6. A number of transitions belonging to sites similar to *B1* and *B3* are believed to be present but are overlapping the  $^7F_0 \rightarrow ^5D_1$  excitation lines of the *C* and *A* sites. The  $^7F_0 \rightarrow ^5D_0$  transitions of two of these poorly characterized sites fall within the inhomogeneous width of the region labeled "p" in Fig. 2(e).

$^7F_0 \rightarrow ^5D_1$  excitation spectra for sites *D1*, *D2*, *E1*, and *E2* are shown in Fig. 3. These sites are assigned to clusters of  $\text{Eu}^{3+}$  ions based on their short  $^5D_1$  lifetimes, concentration dependences, and spectral features. Only three lines are observed in the  $^5D_1$  excitation spectrum for all four of these clusters. Examination of individual-site

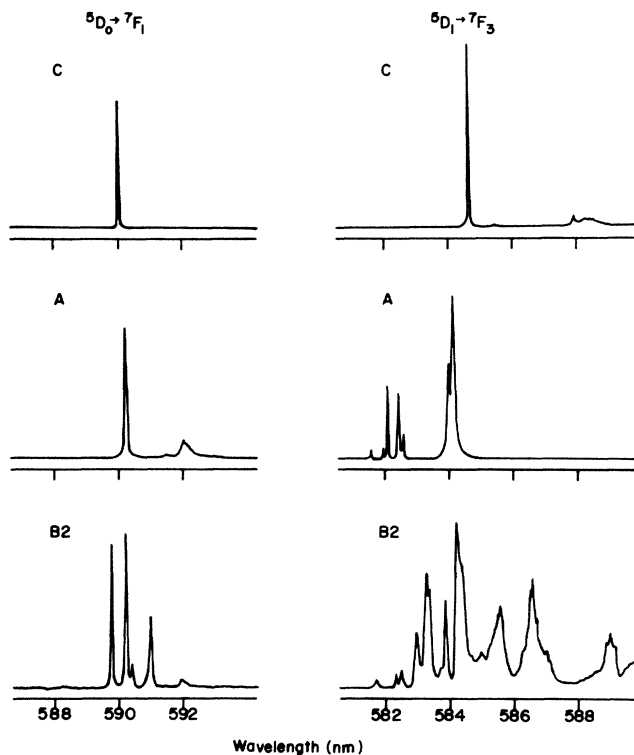


FIG. 4.  $^5D_0 \rightarrow ^7F_1$  and  $^5D_1 \rightarrow ^7F_3$  fluorescence spectra of single-pair sites using the following excitation wavelengths: site *C*, 525.03 nm; site *A*, 578.5 nm (left), 525.08 nm (right); site *B2*, 578.3 nm (left), 525.7 nm (right).

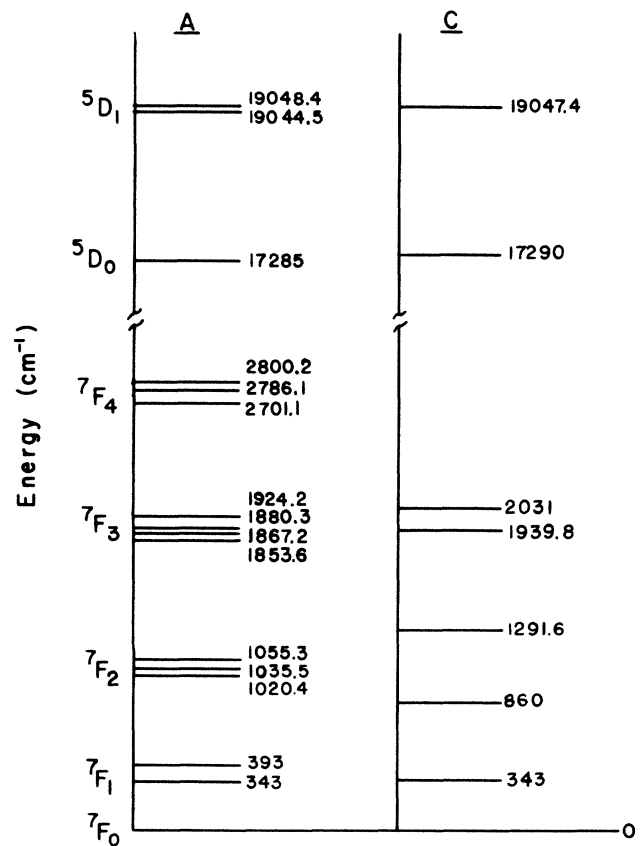


FIG. 5. Energy level of *A* and *C* sites.

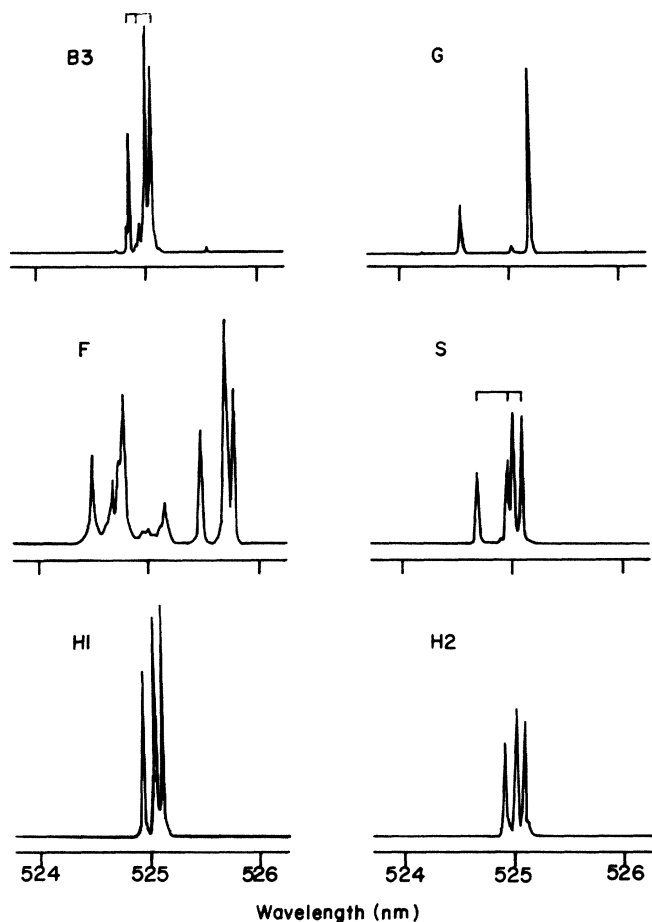


FIG. 6.  ${}^7F_0 \rightarrow {}^5D_1$  excitation spectra of sites in  $\text{PbF}_2:\text{Eu}^{3+}$  monitoring the following wavelengths: site B3, 589.4 nm; site G, 533.8 nm; site F, 586.8 nm; site S, 588.6 nm; site H1, 589.4 nm; site H2, 589.3 nm.

spectra show the position of these transitions for sites D1 and D2 are shifted to higher energies of sites E1 and E2. A difference is also observed in the fluorescent lifetime behavior of these sites. The  ${}^5D_1$  lifetimes are longer and the  ${}^5D_0$  lifetimes are somewhat shorter for sites D1 and D2 relative to sites E1 and E2 (Table I). Under suitable annealing conditions, the D1 and D2 sites may be studied in the 0.1-mol % crystals but they normally have very low intensity. No other sites associated with clusters have been identified in the 0.1-mol % crystal. Our observations suggest that D1 and D2 are  $\text{Eu}^{3+}$  dimers and E1 and E2 are either dimers or higher-order clusters. The F site has the same lifetimes as the D2 site but has seven lines in the  ${}^5D_1$  excitation spectrum. It is the only higher-order cluster reported in this work.

#### Concentration and temperature dependence

Figure 2 shows the qualitative effects of concentration on the  $\text{Eu}^{3+}$  site distribution. The C and A sites are the only dominant sites in the 0.01- and 0.1-mol % crystals. There are a number of minor sites that appear in the 0.1-mol % crystal including the D1, D2, B2, and B3 sites. The D1 and D2 sites can be enhanced by annealing at

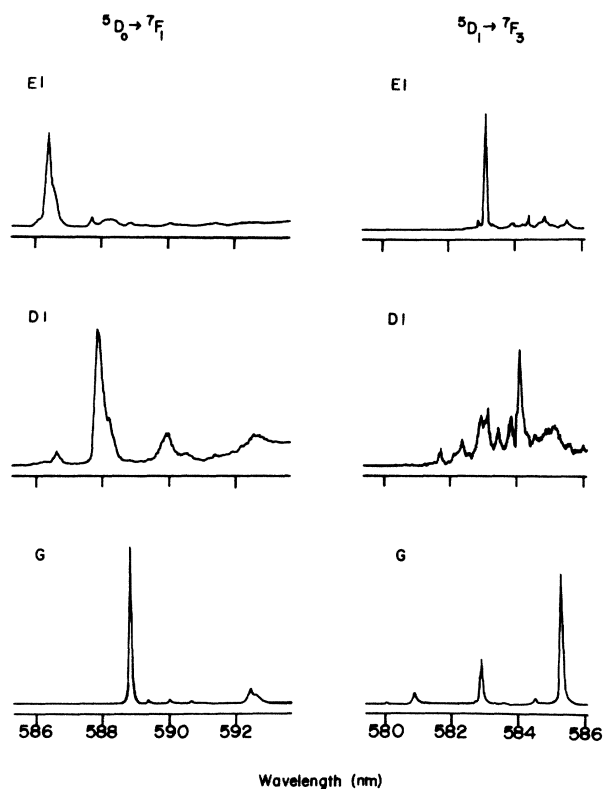


FIG. 7.  ${}^5D_0 \rightarrow {}^7F_1$  and  ${}^5D_1 \rightarrow {}^7F_3$  fluorescence spectra of sites in  $\text{PbF}_2:\text{Eu}^{3+}$  using the following excitation wavelengths: site E1, 577.4 nm (left), 525.7 nm (right); site D1, 579.4 nm (left), 525.6 nm (right); site G, 576.7 nm (left), 524.5 nm (right).

400°C, but regardless of temperature all four sites remain minor sites. The site distribution in the 1.0-mol % crystal reflects the greater importance of clustering, particularly in the  ${}^7F_0 \rightarrow {}^5D_0$  excitation spectrum, but the C and A sites remain important sites.

In order to determine the importance of the C site, the concentrations were determined in the three samples by absorbance measurements. The proportionality constant required to obtain an absolute concentration was measured in a 0.01-mol % crystal annealed at 500°C. At this temperature, all other sites have negligible concentrations and the C site is the only site of importance. The value can then be used to obtain the absolute concentrations of the C site in the other crystals. The absolute C-site concentration increased with total  $\text{Eu}^{3+}$  concentration, but the ratio of C site to total  $\text{Eu}^{3+}$  declined from 0.8 in the 0.01-mol % crystal to 0.4 in the 1-mol % crystal. These values were determined for crystals annealed at 380°C. The relative intensity of the C- and A-site absorption and excitation lines remains relatively constant over the concentration range studied.

The relative importance of  $\text{Eu}^{3+}$  sites in  $\text{PbF}_2$  is sensitive to annealing temperature. In the 0.01- and 0.1-mol % crystal, this dependence manifests itself as a rapid increase of C-site intensity and a rapid decrease in the other sites over a narrow temperature range. In the 1.0-mol % crystal, the changes are less dramatic with the D and E sites gradually declining in importance as annealing tem-

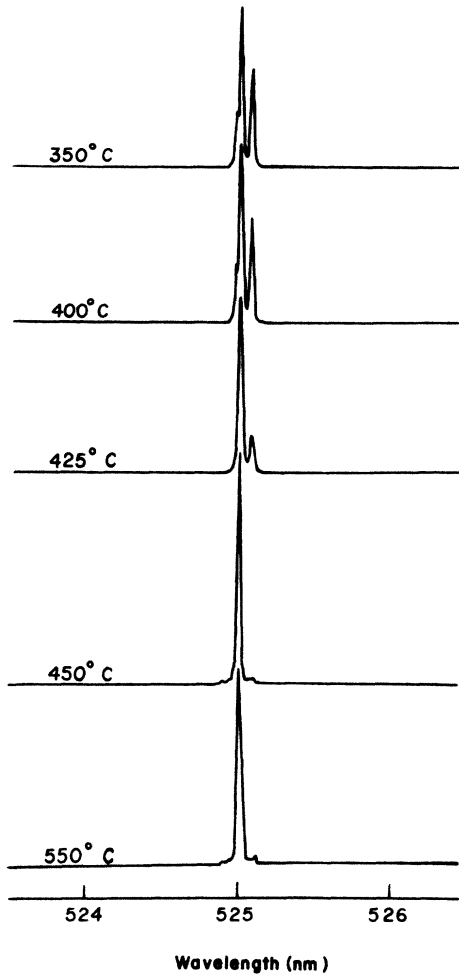


FIG. 8. Dependence of the  ${}^7F_0 \rightarrow {}^5D_1$  excitation spectrum in  $\text{PbF}_2:0.01 \text{ mol } \% \text{ Eu}^{3+}$  on annealing temperature.

perature is increased. Changes in the  ${}^7F_0 \rightarrow {}^5D_1$  excitation spectra for the three concentrations studied at several annealing temperatures are shown in Figs. 8–10. The rapid increase in *C*-site concentration occurs at essentially the same temperatures reported for  $\text{PbF}_2:\text{Er}^{12}$ . The lowest annealing temperatures enhance the formation of the cluster sites.

The temperature dependence of the site distribution in the 1.0-mol % crystal is different from the lower concentrations. At 350°C, the *E1*, *E2*, and *F* clusters have the same importance as the *C* site (Fig. 10). The *F* site rapidly decreases in intensity as annealing temperature increases. It is quite unimportant above 450°C. *E1* and *E2* also decrease in intensity at higher annealing temperatures, rapidly at first, then more slowly above 450°C. Sites *D1* and *D2* have little importance at 350°C. They then increase with annealing temperature until reaching a maximum at 400 to 450°C. At still higher temperatures, the *D* sites decline slowly at the same rate as sites *E1* and *E2*.

The minor single-pair sites also change with temperature in the 1.0-mol % sample. The *B2* site simply decreases with increasing annealing temperature. It has approximately the same intensity as *D1* at most annealing

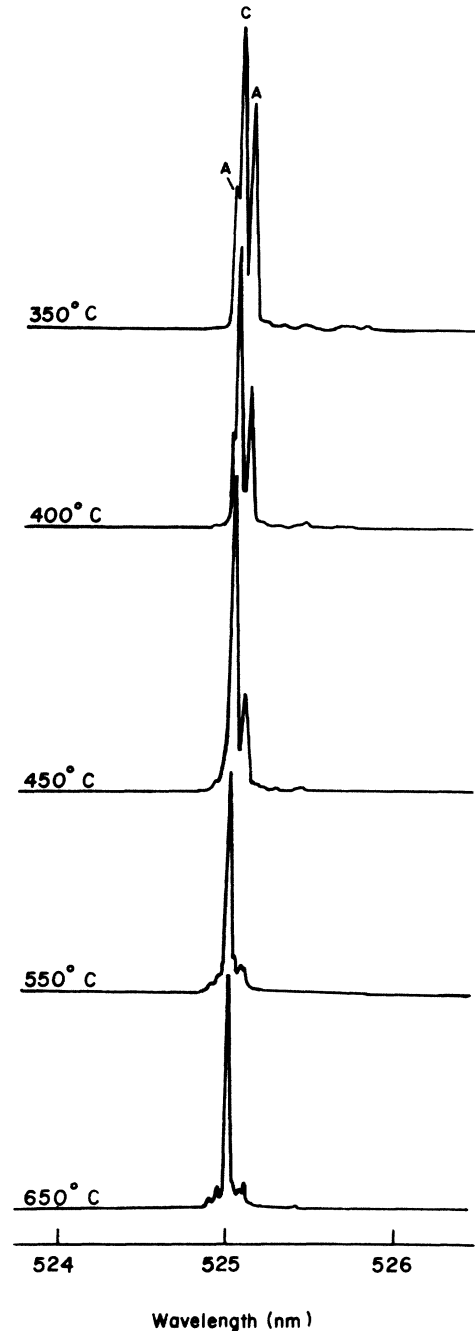


FIG. 9. Dependence of the  ${}^7F_0 \rightarrow {}^5D_1$  excitation spectrum in  $\text{PbF}_2:0.1 \text{ mol } \% \text{ Eu}^{3+}$  on annealing temperature.

temperatures. The *B3* site was not studied in the 1.0-mol % crystal. In the 0.1-mol % crystal *B3* increased to a maximum between 400 and 500°C and then decreased rapidly in intensity with temperature. Even at the maximum, it is considered a minor site in the 1.0-mol % crystal. Site *B1* was not studied in the 0.1-mol % crystal and is a minor site in the 1.0-mol % sample. The annealing behavior of *B1* was not examined. The single-ion sites excited near the region labeled *p* in Fig. 2(e) were not carefully examined. At least one of these sites exists in the 0.1-mol % sample and several exist in the 1.0-mol % sample. They remain minor sites in any of the crystals and

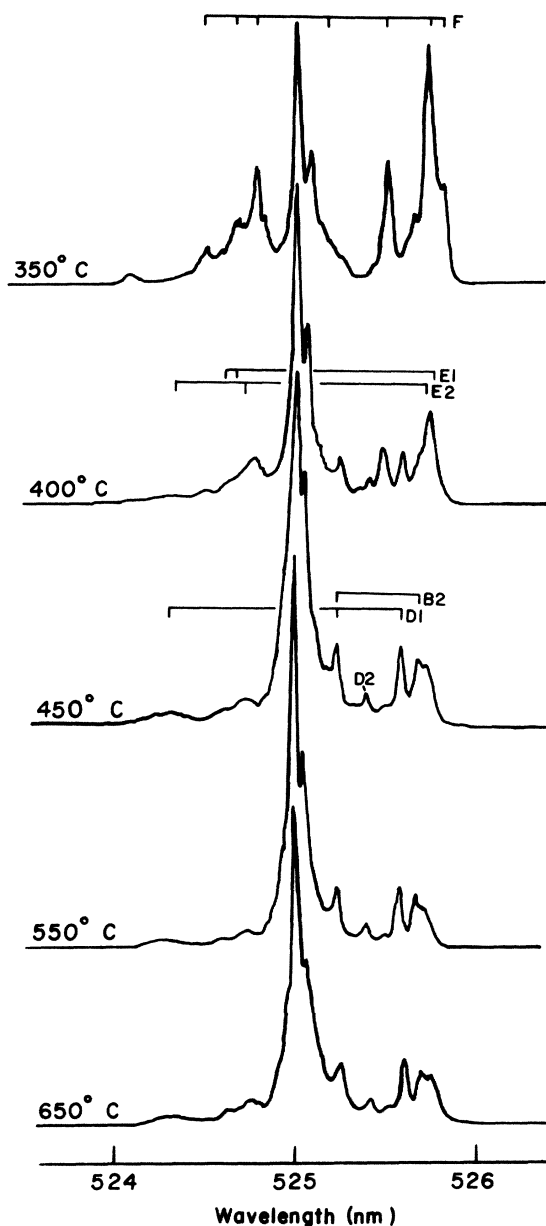


FIG. 10. Dependence of the  ${}^7F_0 \rightarrow {}^5D_1$  excitation spectrum in  $\text{PbF}_2:1.0 \text{ mol } \% \text{ Eu}^{3+}$  on annealing temperature.

were not studied in detail. All of these sites decrease with annealing temperature.

Not all  $\text{Eu}^{3+}$  ions are converted to the *C* site at high temperatures in the 0.1- and 0.01-mol % samples. The weak transitions near the base of the strong *C*-site transition in the high-temperature  ${}^5D_1$  excitation spectra (Figs. 8 and 9) have been assigned to sites *S*, *G*, *H1*, and *H2*. These sites are only observed after annealing above 400°C. At first it was thought these sites may have been due to contaminants introduced during the annealing procedure. However, the sites could be removed from the spectrum by heating the sample to 700°C and allowing it to cool at a controlled rate over a two day period as was done in the original sample preparation procedure. It is unlikely that a contaminant could be added reversibly. The *H1* and *H2*

sites are very similar. They have nearly identical fluorescent lifetimes and the positions of their three  ${}^7F_0 \rightarrow {}^5D_1$  and  ${}^5D_0 \rightarrow {}^7F_1$  transitions differ by approximately  $1 \text{ cm}^{-1}$ . The *S* site is puzzling because it has an extremely fast  ${}^5D_1$  lifetime suggesting assignment as a multiple-ion site. It is unexpected that such a site would be stable only at high temperature. Of the four minor high-temperature sites, only the *G* site has an observable  ${}^7F_0 \rightarrow {}^5D_0$  transition. The position of this transition falls within the inhomogeneous width of *p* region in Fig. 2(e). The line assigned to the *G* site in the  ${}^7F_0 \rightarrow {}^5D_0$  excitation spectrum is the only line to increase in importance as annealing temperature is increased.

#### DISCUSSION AND CONCLUSIONS

The absorption spectra of the low-concentration crystals show only the *A* and *C* sites. This observation is important in ruling out the possibility of having an electron-compensated site that escaped detection by site-selective spectroscopy because its fluorescence was quenched by energy transfer to the electron. A unique correspondence was established between the three dominant dielectric peaks in  $\text{PbE}_2:\text{Er}^{3+}$  and the sites observed by site-selective spectroscopy.<sup>25</sup> Two of these sites were single pairs and the third was associated with clustering. The optical spectroscopy shows  $\text{PbF}_2:\text{Eu}^{3+}$  is very similar but there are fewer sites. Only one important single-pair site is observed and the clustering is not as important until higher concentrations are reached. The optical spectra would therefore predict that only one site would contribute to the dielectric relaxation at low concentrations as is in fact observed.<sup>1</sup> The dielectric relaxation measurements and the spectroscopic measurements are thus in agreement if one assigns the single dielectric peak to the *A* site.

In order to correlate the optical spectrum with the dielectric relaxation measurements, the dielectric relaxation of 0.1-mol %  $\text{PbF}_2:\text{Eu}^{3+}$  crystals annealed at 384, 450, and 550°C was measured and compared with the optical spectra for the same crystals. The results are shown in Fig. 11. These should be compared with the optical results shown in Figs. 2(d) and 9. The behavior of the *A* site and the dielectric peak correlate excellently and show that they correspond to the same site.

The spectra of the *A* site and its dependence on dopant concentration and annealing temperature are so similar to the other fluorites and to  $\text{PbF}_2:\text{Er}^{3+}$  (Ref. 25) that the compensation mechanism must be a  $F_i^-$  and not an electron. Indeed, since the *A* site dissociates at temperatures around the superionic transition, there would have to be a large component in the conductivity resulting from the charge compensation. Since the conductivity has been shown to be primarily ionic and described by a classical association model,<sup>17</sup> the charge compensation must be a  $F_i^-$ . Such an assignment was an alternative model suggested by Fontanella *et al.*<sup>1</sup> The failure of the conductivity to scale with the size of the relaxation peak would then be attributed to a large association energy for the site. A large association energy, however, would seem to be in disagreement with the fact that the bulk conductivity is described by a classical association model. The discrepan-

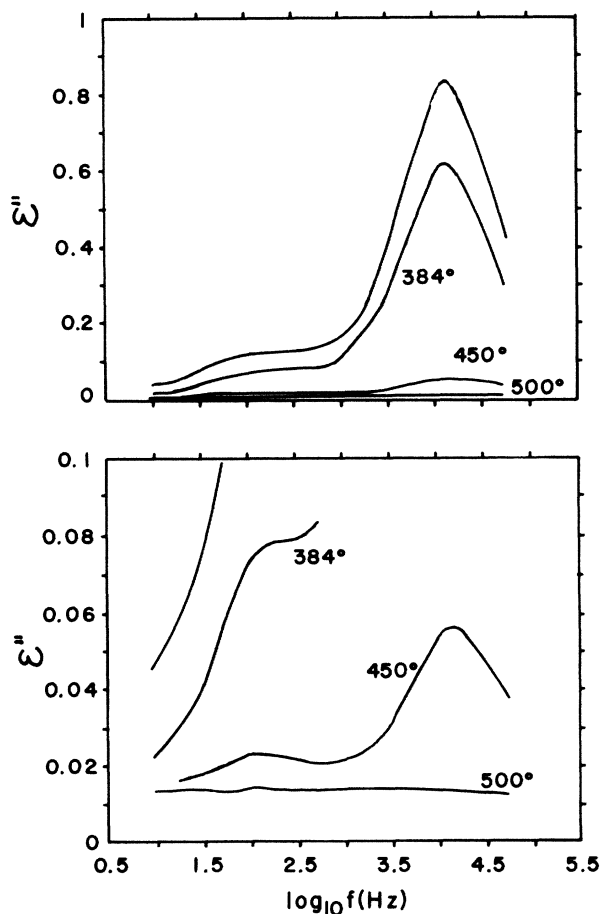


FIG. 11. The dielectric relaxation for  $\text{PbF}_2:0.1 \text{ mol } \% \text{Eu}^{3+}$  crystals that were cooled slowly after growth (top curves) or annealed at 384, 450, and 550°C. The results are shown for two different sensitivities.

cy was previously resolved by postulating the existence of another site that was invisible to the dielectric relaxation but could dissociate and contribute to the conductivity.<sup>1</sup> Our data shows that there is no candidate for such a site and the *A* site must correspond to the one that contributes to the conductivity in the classical association model. The discrepancy can be considered as additional evidence for the importance of the nonidealities in the fluorites that have been observed in many other studies.<sup>20,21,23,25</sup>

It has been suggested that simple mass action relationships do not describe the defect equilibria in the fluorites because of interactions between defects. These interactions are usually considered to be Coulombic in nature but recent evidence suggests there is a large contribution from the mechanical strains induced in the lattice from the

dopants.<sup>23,25</sup> The strains are minimized by a nonrandom distribution of the defects that mimics the distribution caused by Coulombic interactions. The nonrandom distribution causes increased shielding and enhances the dissociation of the single pairs. It has been argued that this effect is one of the driving forces for the superionic transition.<sup>25</sup> Higher temperatures cause a greater number of defects which causes more strains and a greater shielding. One can see the association energy would not be independent of the temperature of the crystal and could be large at the lower temperatures of the dielectric measurements and smaller at the higher temperatures of the conductivity measurements. The temperature dependence of the *A* site is so strong around the superionic transition that a unique activation energy could not explain the sudden dissociation. Thus it is argued that the nonideality effects associated with the superionic conductivity are necessary to explain the failure of the conductivity to scale with the size of the dielectric relaxation peak.

The nonidealities must certainly be responsible for the strong temperature dependence of the *A* site and cubic site around the superionic transition temperature. Fluoride interstitials are mobile at room temperature and would be able to combine with  $\text{Eu}^{3+}$  ions in cubic sites if it was favorable to do so. The fact that they do not indicates that there has been a change in the formation energies that makes the recombination unfavorable. The dissociation of the clusters could cause an increase in the strains in the lattice that are responsible for the large nonideality correction and the resulting change in the associated to dissociated site ratio.

The strain interactions may also be responsible for the shift in the activation energy of the dielectric peak.<sup>1</sup> The large shifts observed in  $\text{PbF}_2$  and the lack of shifts in the alkaline-earth fluorides may reflect the greater importance of the strain interactions in  $\text{PbF}_2$ . The greater effects of strains may be an important factor in making  $\text{PbF}_2$  a good superionic conductor. The difference in the behavior of the site distribution with annealing temperature in the 1.0-mol% crystal may also reflect the nonidealities. At these high concentrations, the ions are always relatively close even if the defects were randomly distributed and any interactions between them would promote reassociation. Thus one would not see the locally compensated sites dissociate near the superionic transition at the higher dopant concentrations.

#### ACKNOWLEDGMENTS

This work was supported by the National Science Foundation under Grant Nos. DMR-82-05145 and DMR-85-13705.

\*Author to whom correspondence should be sent.

<sup>1</sup>J. J. Fontanella, M. C. Wintersgill, D. R. Figueroa, A. V. Chadwick, and C. G. Andeen, *Phys. Rev. Lett.* **51**, 1892 (1983).

<sup>2</sup>G. A. Samara, *Phys. Rev. B* **13**, 4529 (1976).

<sup>3</sup>G. A. Samara, *Ferroelectrics* **17**, 357 (1977).

<sup>4</sup>M. O. Manasreh and D. O. Pederson, *Phys. Rev. B* **30**, 3482 (1984).

<sup>5</sup>C. E. Derrington, A. Navrotsky, and M. O'Keeffe, *Solid State Commun.* **18**, 47 (1976).

<sup>6</sup>J. J. Fontanella, M. C. Wintersgill, P. J. Welcher, A. V. Chadwick, A. Azimi, V. M. Carr, and C. G. Andeen, in *Stud-*

- ies in Inorganic Chemistry*, Vol. 3 of *Solid State Chemistry 1982, Studies in Inorganic Chemistry*, edited by R. Metselaar and H. J. M. Heijligers (Elsevier, Amsterdam, 1983).
- <sup>7</sup>M. C. Wintersgill, J. J. Fontanella, F. P. Pursel, A. V. Chadwick, A. Azimi, V. M. Carr, and C. G. Andeen, *Radiat. Eff.* **75**, 263 (1983).
- <sup>8</sup>N. Suarez, D. Figueroa, E. Laredo, and M. Puma, *Cryst. Lattice Defects* **9**, 207 (1982).
- <sup>9</sup>C. Andeen, D. Link, and J. Fontanella, *Phys. Rev. B* **16**, 3762 (1977).
- <sup>10</sup>C. G. Andeen, J. J. Fontanella, M. C. Wintersgill, P. J. Welcher, R. J. Kimble, Jr., and G. E. Matthews, Jr., *J. Phys. C* **14**, 3557 (1981).
- <sup>11</sup>C. G. Andeen, G. E. Matthews, Jr., M. K. Smith, and J. J. Fontanella, *Phys. Rev. B* **19**, 5293 (1979).
- <sup>12</sup>J. J. Fontanella, M. C. Wintersgill, and C. G. Andeen, *Phys. Status Solidi B* **97**, 303 (1980).
- <sup>13</sup>C. G. Andeen, J. J. Fontanella, and M. C. Wintersgill, *J. Phys. C* **13**, 3449 (1980).
- <sup>14</sup>M. C. Wintersgill, J. J. Fontanella, P. Welcher, R. J. Kimble, Jr., and C. G. Andeen, *J. Phys. C* **13**, L661 (1980).
- <sup>15</sup>J. J. Fontanella, M. C. Wintersgill, A. V. Chadwick, R. Saghafian, and C. G. Andeen, *J. Phys. C* **14**, 2451 (1981).
- <sup>16</sup>J. Schoonman, G. A. Korteweg, and R. W. Boone, *Solid State Commun.* **16**, 9 (1975).
- <sup>17</sup>R. W. Boone and J. Schoonman, *J. Electrochem. Soc.* **124**, 28 (1977).
- <sup>18</sup>D. R. Tallant and J. C. Wright, *J. Chem. Phys.* **63**, 2075 (1975).
- <sup>19</sup>M. D. Kurz and J. C. Wright, *J. Lumin.* **15**, 169 (1977).
- <sup>20</sup>D. S. Moore and J. C. Wright, *J. Chem. Phys.* **74**, 1626 (1981).
- <sup>21</sup>R. J. Hamers, J. R. Wietfeldt, and J. C. Wright, *J. Chem. Phys.* **77**, 683 (1982).
- <sup>22</sup>S. I. Mho and J. C. Wright, *J. Chem. Phys.* **77**, 1183 (1982).
- <sup>23</sup>J. C. Wright, in *Crystal Lattice Defects and Amorphous Materials* [Cryst. Lattice Defects Amorph. Mater. **12**, 505 (1985)].
- <sup>24</sup>J. P. Jouart, C. Bissieux, G. Mary, and M. Egee, *J. Phys. C* **18**, 1539 (1981).
- <sup>25</sup>S. I. Mho and J. C. Wright, *J. Chem. Phys.* **79**, 3962 (1983).
- <sup>26</sup>M. P. Miller, D. R. Tallant, F. J. Gustafson, and J. C. Wright, *Anal. Chem.* **49**, 1474 (1977).
- <sup>27</sup>P. R. Findely, Z. Wu, and W. C. Walker, *Solid State Ionics* **7**, 49 (1982).
- <sup>28</sup>C. R. A. Catlow, *J. Phys. C* **9**, 1845 (1976).